Autopilot Design for Agile Initial Pitch-over Maneuver Using Schmitt-trigger

Ju-Hyeon Hong[1] and Gwanyong Moon[2]

Abstract— **The proposed autopilot employs a skid-to-turn scheme to achieve a faster time response. The pitch and yaw channel autopilots utilize a two-loop design, incorporating a PI (Proportional-Integral) controller in the inner loop to track the angular rate command and a Schmitt trigger in the outer loop. The Schmitt trigger determines the direction of rotation for rapid attitude changes. A precomputed table generates the maximum normal acceleration, which defines the amplitude of the angular rate command. This combination of the Schmitt trigger and the maximum trim command ensures stability and maximizes maneuverability during the initial pitch-over phase. Although the skid-to-turn approach may result in larger tracking errors compared to bank-to-turn methods, it still achieves the primary objective of a fast time response during the initial pitch-over phase. The effectiveness of the autopilot is validated through non-linear 6-DOF simulations and Monte Carlo simulations that account for aerodynamic uncertainties.**

I. INTRODUCTION

Highly maneuverable missiles require agile turning capability, particularly in the initial phase, to align with the target's incoming direction. During this phase, the missile's speed has not yet built up, and aerodynamic forces are insufficient to ensure high maneuverability. In such cases, thrust vectoring provides additional control force and moment, enabling the missile to rapidly pitch over while operating in a low dynamic pressure region. Among various thrust vectoring methods, a relatively simple and effective solution is placing jet vanes in the exhaust plume of the main thruster to deflect the thrust vector[1]. Four jet vanes can simultaneously generate roll, pitch, and yaw control forces and moments, making this an effective method for controlling the vehicle during rapid pitch-over maneuvers immediately after launch[2].

To achieve a fast pitch-over maneuver, the autopilot must account for the highly nonlinear and rapidly changing missile dynamics. One dominant source of nonlinearity is jet vane erosion, which occurs due to prolonged exposure to high-temperature gases, unpredictably altering its physical properties. Therefore, completing the initial pitch-over maneuver before significant erosion begins is crucial. Additionally, since rapid maneuvers, such as the fast pitch-over motion, require a high angle of attack, the aerodynamic characteristics at high angles of attack must also be taken into account when designing the autopilot to maintain stability[3]. These nonlinearities present challenges in developing an agile and stable autopilot for air-launched missiles.

Moreover, the cross-coupling effects between the pitch and yaw control channels add complexity that must be managed for effective maneuvering. Specifically, roll aerodynamics are highly nonlinear and depend on incidence and sideslip trim in the high-angle-of-attack region, further complicating the design of a bank-to-turn autopilot structure. In this context, the skid-to-turn scheme, which decouples yaw and pitch dynamics, offers advantages by avoiding complications from roll coupling effects. This approach focuses on pitch-over motion without inducing roll during the short boosting phase.

The literature on designing autopilots for agile-turn missile control primarily employs nonlinear control theories. The nonlinear backstepping approach is proposed to stabilize the system while addressing uncertainties and delays through time-delay adaptation. Optimal angle-of-attack (AOA) profiles, which maximize agile-turn performance, serve as reference commands for the controller.[4], [5]. The robust H-infinity control method is also considered for agile missiles [6]. Additionally, the feedback linearization method transforms the nonlinear system into an equivalent linear system, enabling the use of linear control design techniques, such as the pole placement method[7]. An integrated guidance-autopilot system is designed to coordinate jet-vane thrust vectoring with aerodynamic control surfaces during agile bank-to-turn maneuvers[8], [9]. Overall, advanced nonlinear control techniques with complex structures are proposed to enable precise tracking of the large and rapid angle-of-attack commands required for agile-turn maneuvers in highly maneuverable missiles. Furthermore, previous methods have focused on a single axis, which could serve as a starting point for the skid-to-turn structure or be integrated into the bank-to-turn structure[10], [11], [12].

This paper proposes a novel autopilot structure that integrates aerodynamic control and jet-vane actuation to achieve the initial agility of a skid-to-turn missile. The fundamental control loop, which incorporates aerodynamic characteristics, utilizes a bang-bang type controller derived from a time-optimal solution to mitigate the nonlinear effects caused by jet-vane erosion. Among bang-bang type controllers, this paper adopts the Schmitt trigger method to avoid the chattering phenomenon associated with conventional bang-bang controllers. Additionally, the maximum trimmed angular rate command is pre-calculated based on the maximum lateral acceleration in the trim condition and is used as a key parameter in the control scheme. In summary, the proposed autopilot aims to minimize response time during the initial

*This work was supported by the Agency for Defense Development, Republic of Korea.

[1]Ju-Hyeon Hong is with the Agency for Defense Development in Korea, Deajeon, Republic of Korea hong.ju.hyeon11@gmail.com

[2]Gwanyong Moon is with the Agency for Defense Development in Korea, Deajeon, Republic of Korea rootlocy@gmail.com

pitch-over phase by generating trimmed maximum angular rate commands using a Schmitt trigger.

This paper is organized as follows: Section 2 defines the dynamics model of the skid-to-turn missile. Section 3 introduces the structure and foundational equations of the proposed autopilot, along with an analysis of its stability margin and time response. The proposed method is verified through single-run 6-DOF nonlinear simulations and a Monte Carlo simulation with aerodynamic uncertainties in Section 4. Finally, conclusions are presented in Section 5

II. PROBLEM DEFINITION

Consider a missile equipped with four aerodynamic tail fins and jet vanes. The control moment consists of both the aerodynamic moment and the thrust moment generated by the jet vanes, as the jet vanes and tail fins are coupled and deflected simultaneously. The missile's configuration is shown in Figure 1. The governing equation for the pitch attitude angle of the missile can be simplified and expressed as the following second-order differential equation. Since the pitch and yaw planes are symmetric, their governing equations can be considered equivalent.

Assuming $\alpha = \theta - \gamma$ and $q = \dot{\theta}$, the pitch motion can be described in terms of the rate of angle of attack and pitch rate as follows:

$$\dot{\alpha} = q + Z_\alpha \alpha + (Z_\delta^A + Z_\delta^T)\delta. \tag{1}$$

$$\dot{q} = \frac{1}{I_{yy}}(M^A + M^T) = M_\alpha \alpha + M_q q + (M_\delta^A + M_\delta^T)\delta. \tag{2}$$

where γ, a_m, V_m, and δ represent the flight path angle, normal acceleration, missile speed, and control surface deflection angle, respectively. q, Z^A, M^A, Z^T, M^T, and I_{yy} denote the pitch angular rate, aerodynamic force and moment, thrust force and moment, and moment of inertia about the pitch axis, respectively.

In this study, a nonlinear missile model with a boost phase is considered. The maneuverability requirements for the agile missile include performing a 180-degree turn in the pitch plane after launch. The aerodynamic fins and jet vanes serve as control actuators, being mechanically linked and operated simultaneously.

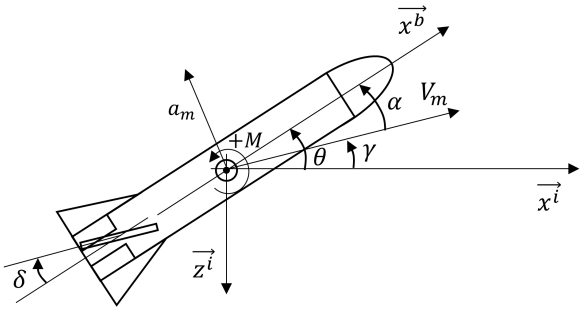

Fig. 1: Configuration of the missile with aerodynamic fins and jet vanes.

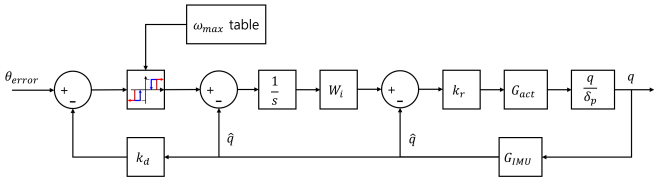

Fig. 2: Structure of the proposed pitch/yaw channel autopilot.

III. AUTOPILOT DESIGN

The proposed autopilot is designed based on a skid-to-turn scheme to achieve a fast time response. The pitch/yaw channel autopilot features an integrated PI controller with a Schmitt trigger method to determine the direction of the angular rate. Since the missile configuration has a symmetric shape along the pitch and yaw axes, the autopilots for the pitch and yaw channels are designed equivalently. The magnitude of the angular rate command is defined by a pre-calculated table that generates the maximum normal acceleration.

A. Basic structure of the proposed autopilot

The overall structure of the proposed pitch/yaw channel autopilot is depicted in Figure 2. The inner loop is designed with a PI controller to track the angular rate command, and the control gains W_i and k_r are determined based on the operational region defined by Mach number and altitude. The outer loop features a pseudo bang-bang nonlinear controller known as the Schmitt trigger, which generates the maximum control command. The Schmitt trigger determines whether the control command is positive, negative, or zero and facilitates switching the direction of the inner loop's control command. The angular rate command in the inner PI controller is defined by a pre-calculated maximum normal acceleration.

B. Schmitt-trigger design

To achieve a fast attitude response for the missile, a bang-bang controller—designed to minimize time—is an optimal choice. However, it inherently exhibits a chattering phenomenon near the desired states. To address this issue, the Schmitt trigger, recognized as a pseudo time-optimal solution, is selected. This approach provides an effective bang-off-bang solution while efficiently handling dead-zone and hysteresis characteristics. The dead-zone helps reduce the effects of noise and disturbances on the trigger, while the hysteresis effect enhances control accuracy. As a result, both accuracy and robustness improve with minimal control input. The structure of the Schmitt trigger is shown in Figure 3.

The input to the Schmitt trigger is the angle error, calculated as the difference between the desired and current attitude angles. The outer loop includes a derivative controller, where the derivative gain k_d is determined to define the range of the dead zone and hysteresis.

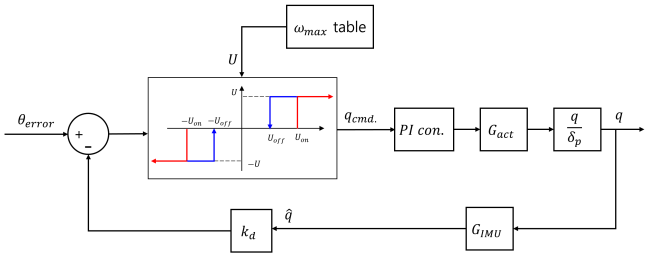

Fig. 3: Structure of the outer loop controller.

The parameters of the Schmitt trigger are determined using the following equations.

$$k_d = \sqrt{\frac{10\chi_0}{M_0}}, \quad \omega_a = M_0 \Delta t_{step}. \tag{3}$$

$$U_{on} = \chi_0 + \omega_a k_d, \quad U_{off} = \chi_0 - \omega_a k_d. \tag{4}$$

where χ_0, M_0, Δt_{step}, and ω_a represent the limits of the attitude angle error, control moment, time step, and internal rate, respectively.

The switching conditions are defined based on U_{on} and U_{off}, and the output of the Schmitt trigger determines the direction of the control command. The input to the Schmitt trigger is given by:

$$U_0 = (\theta_{desired} - \hat{\theta}) - k_d \hat{q}. \tag{5}$$

where $\theta_{desired}$, $\hat{\theta}$, and $\hat{q}$ represent the desired pitch angle, the current pitch angle, and the current pitch angular rate, respectively.

An example of the tracking performance of the Schmitt trigger is shown in Figure 4. In this figure, the blue line represents the time response of the basic control using a derivative controller, which shares the same control gains k_d as the outer loop. The red line illustrates the time response of the outer loop with the Schmitt trigger. The accuracy parameter χ_0 is set to 0.05, ensuring that the tracking error remains within ±5%, as depicted in Figure 4.

C. Pre-calculated maximum acceleration table

To determine the magnitude of the control command, the maximum normal acceleration is calculated based on the trim

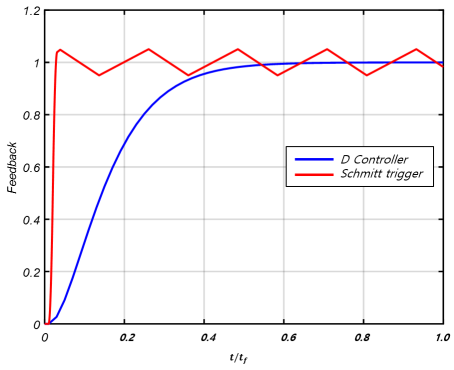

Fig. 4: Example of time response for the outer loop.

condition. The process begins by finding the trim deflection angles required to maintain zero moments across all three axes. At each operational point, these trim deflection angles are determined, allowing the trim lateral force coefficients for the pitch and yaw channels to be expressed by the following equation.

$$C_y = C_{y0}^A + C_{y\delta_r}^A + C_{y\delta_y}^A + C_{y\delta_p}^A + C_{y\delta_y}^T. \tag{6}$$

$$C_z = C_{z0}^A + C_{z\delta_r}^A + C_{z\delta_y}^A + C_{z\delta_p}^A + C_{z\delta_p}^T. \tag{7}$$

where C_{y0}^A, $C_{y\delta_r}^A$, $C_{y\delta_y}^A$, $C_{y\delta_p}^A$, C_{z0}^A, $C_{z\delta_r}^A$, $C_{z\delta_y}^A$, and $C_{z\delta_p}^A$ are the lateral force coefficients due to aerodynamic forces, while $C_{y\delta_y}^T$ and $C_{z\delta_p}^T$ are the lateral force coefficients generated by the jet vanes.

Figure 5 shows the control moment coefficients generated by the aerodynamic fins and jet vanes. In this figure, the x-axis represents the normalized speed, while the y-axis represents the control moment coefficients. The jet-vane control moment coefficient remains steady as the speed increases, while the aerodynamic control moment coefficient exhibits a sharp gradient with increasing missile speed. The coefficients labeled M_δ^{vane} : *ideal* (without erosion) are larger than those labeled M_δ^{vane} : *Erosion*30%, which are calculated using the erosion model for the jet-vane area. Since the control effectiveness of the jet vane depends on the main thruster's burning time and the nonlinear effects caused by erosion, the pitch-over maneuver using the jet vane must be completed as early as possible to maximize the available control moments while minimizing nonlinear effects. Although the use of jet vanes comes with certain constraints, combining the control moments generated by both the jet vane and aerodynamic fins enables the missile to achieve sufficient control authority. This approach significantly expands the operational region for executing the initial pitch-over maneuver compared to using aerodynamic control alone. The lateral acceleration generated by the combined effects of the aerodynamic fins and jet vane can be expressed as follows:

$$a_{my} = \frac{QSC_y}{m}, \quad a_{mz} = \frac{QSC_z}{m}. \tag{8}$$

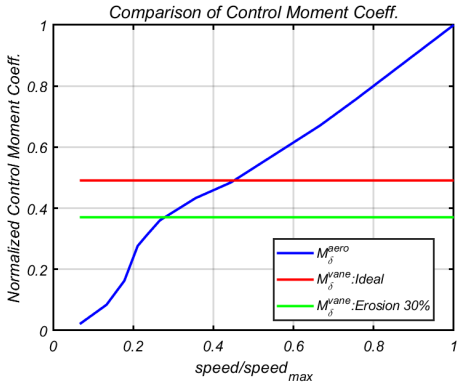

Fig. 5: Comparison of control moment coefficients between aerodynamic fins and jet vanes.

where Q, S, and m represent the dynamic pressure, reference area, and missile mass, respectively.

The total acceleration at each operational point can be expressed as a function of the angle of attack α, sideslip angle β, Mach number M, and altitude h as follows:

$$a_m(\alpha,\beta,M,h) = \sqrt{a_{my}^2 + a_{mz}^2}. \tag{9}$$

To determine the maximum acceleration, the total acceleration table can be simplified into a two-dimensional table as a function of Mach number and altitude at each operational point. Consequently, the maximum acceleration can be obtained as follows:

$$a_{max}(M,h) = \max\left(a_m(\alpha,\beta,M,h)\right). \tag{10}$$

It is important to note that the maximum acceleration is typically determined under the maximum trimmed angle of attack condition. In this context, the maximum acceleration can be converted into the maximum angular rate using the flight path angle rate equation, Eq.(1) as follows:

$$q_{desired} = \frac{a_{max}}{\sqrt{2}V_m}. \tag{11}$$

Since a_{max} is the total acceleration, defined as the root-sum-square of the accelerations in pitch and yaw axes, the geometric factor $1/\sqrt{2}$ is applied in Eq. (14) to account for using only the pitch command. Additionally, assuming $q \sim \dot{\gamma}$, the pitch rate command can be obtained from $\dot{\gamma} = \frac{a}{V_m}$.

The desired pitch angular rate $q_{desired}$ will be used to define the magnitude of the outer loop.

D. Inner PI controller design

The structure of the inner loop controller, based on Nesline's three-loop autopilot[13], is shown in Figure 6. The control gains k_p, W_i, and k_r are selected with consideration for the stability margin and time response. After determining the gains, W_i and k_r are used in the inner PI loop of the autopilot, while the outer proportional k_p is replaced by a control loop containing the Schmitt trigger, as shown in Figure 3. The outer loop with gain k_p is applied after completing the initial pitch-over phase to stabilize the missile's attitude before transitioning to the mid-course guidance phase.

The goals of gain tuning are as follows:

- Gain margin $>$ 6 dB
- Phase margin $>$ 30 deg
- Rise time (90%) $<$ 0.2 t/t_f

In Figure 7, M1 represents the speed, while H1, H2, and H3 correspond to low, middle, and high altitude conditions, respectively. Various angles of attack and sideslip angles are set to evaluate the stability margin and time response at each

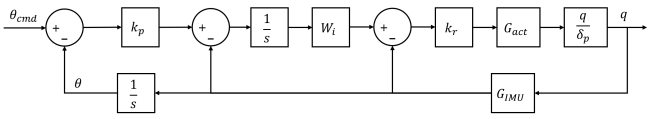

Fig. 6: The structure of the inner loop.

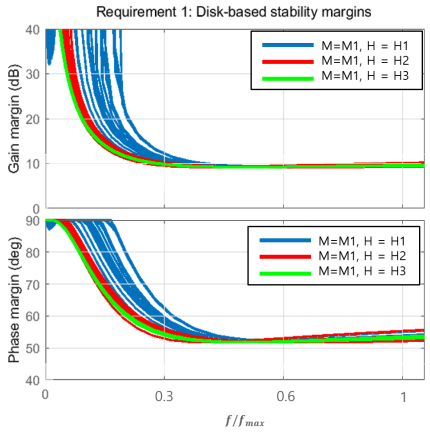

(a) The stability margins.

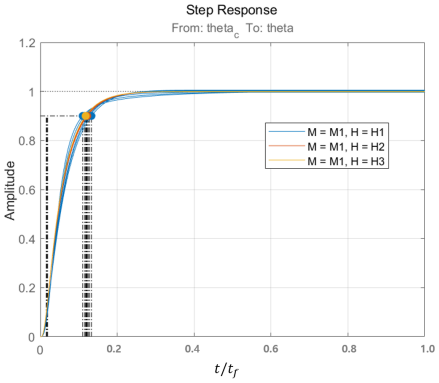

(b) The time response.

Fig. 7: Performance of the inner loop.

point. Figure 7a depicts the stability margins of the inner loop, verified at 12 separate design points. At all design points, the gain margin exceeds 6 dB, and the phase margin exceeds 40 degrees. These results indicate that the proposed control system satisfies the design goals with appropriate stability margins. The design points at high altitude show consistent margins across various angles of attack, while those at low altitude exhibit significant variation in the low-frequency region, suggesting that aerodynamic effects are dominant in the low-altitude region.

The time response of the inner loop is verified in Figure 7b. All step responses indicate that the 90% rise time is under 0.2 t/t_f, meeting one of the design goals. The overshoot is also less than 3%, and the time responses are well-damped. Additionally, the settling times are under 0.3 t/t_f, and the steady-state error is near zero. The linear analysis confirms the performance of the inner loop controller in terms of both stability and time response, demonstrating that the design goals are fully achieved.

IV. SIMULATION RESULTS

To evaluate the performance of the proposed autopilot, a nonlinear missile model equipped with aerodynamic fins and jet vanes is implemented within a 6-DOF simulation environment. The maneuverability requirements for the agile

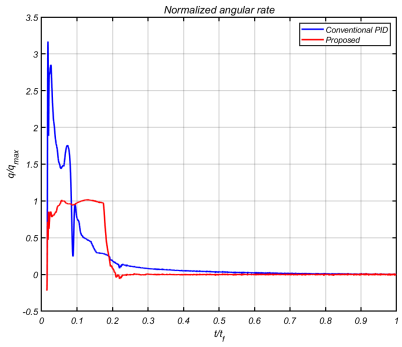

(a) Normalized angular rate.

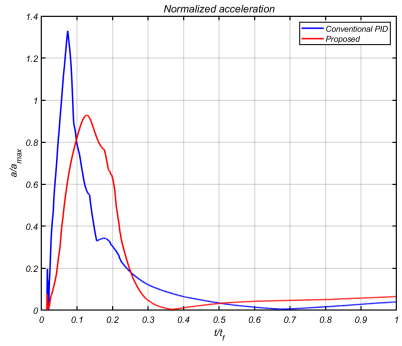

(b) Normalized acceleration.

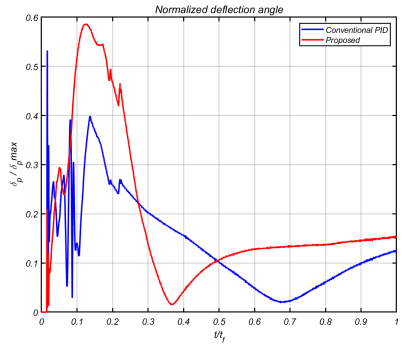

(c) Normalized deflection angle.

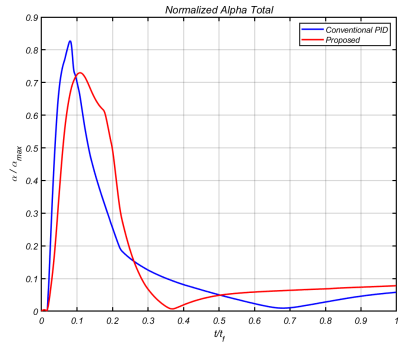

(d) Normalized total angle of attack.

Fig. 8: Normalized single run results.

missile include executing a 180-degree turn in the pitch plane after launch, which drives the pitch angle command to facilitate this maneuver.

The roll channel autopilot is designed using the conventional structure shown in Figure 6, while the pitch and yaw channel autopilots employ the proposed agile autopilot structure depicted in Figure 2. The initial pitch angle is set to 0 degrees, with the target pitch angle at 180 degrees. The initial pitch-over phase ends when the jet vanes, effective only during the boost phase, provide the missile with additional control moments.

The performance of the proposed autopilot is compared to a conventional PID attitude loop. The x-axis of Figures 8 represents the normalized flight time. The normalized angular rate is shown in Figure 8a, with the maximum pitch rate calculated using Eq.(11), which represents the inner loop's command. The pitch angular rate remains stable, and the tracking error of the angular rate stays within 10% during the pitch-over maneuver. The normalized acceleration increases to achieve the maximum turning rate under the trim condition, as illustrated in Figure 8b. The deflection angle, depicted in Figure 8c, remains below 0.6. Additionally, as shown in Figure 8d, the missile attempts to utilize the maximum angle of attack during the initial pitch-over phase, with the ratio approaching 1. This indicates that the proposed autopilot maintains stability in the high angle of attack region as well.

Figure 9a illustrates the pitch angle, which effectively converges to the command with the maximum turn rate while

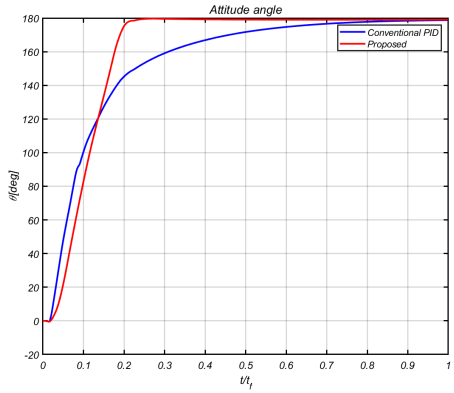

(a) Pitch angle histories.

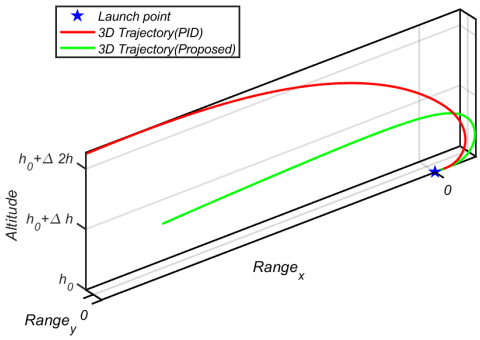

(b) Trajectory in 3D Plane.

Fig. 9: Attitude angle histories and trajectories.

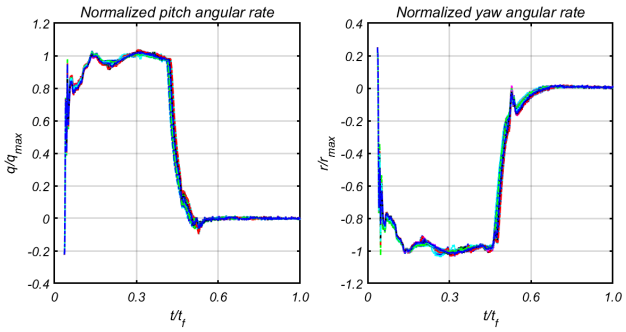

(a) Normalized angular rates.

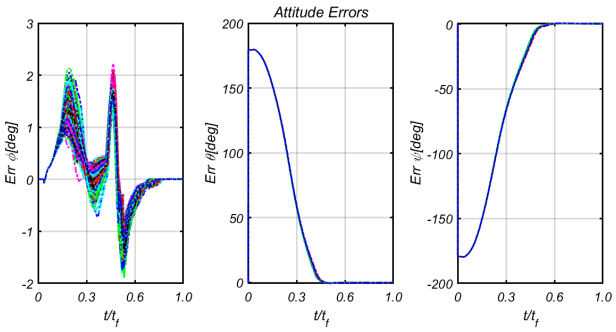

(b) Attitude error histories.

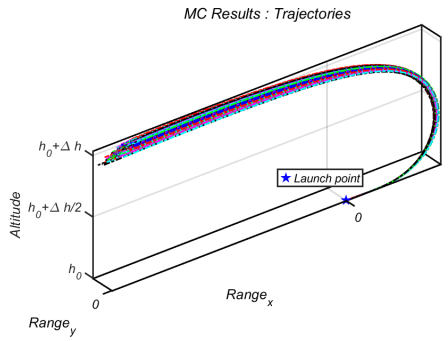

(c) 3D trajectories.

Fig. 10: Monte-Carlo simulation results.

maintaining stability. The angle error also converges before 0.2 t/t_f, as intended. Finally, Figure 9b presents the 3D trajectory of the pitch-over maneuver, demonstrating stable attitude and position in the 3D plane, with all axes of the trajectory scaled equally. This result shows that the turning radius of the proposed algorithm is less than half that of the conventional approach, indicating that the proposed control scheme enables rapid agile turns.

It is worth mentioning that the proposed method uses the pre-calculated maximum acceleration under a trim condition, which is sensitive to aerodynamic uncertainties. To verify the performance of the proposed structure under these uncertainties, a Monte Carlo simulation is performed with aerodynamic coefficient errors that follow a normal distribution. As shown in Figure 10a, the angular rate exhibits chattering near the maximum angle of attack regions. However, the attitude error angles, depicted in Figure 10b, converge to zero smoothly. Moreover, the pitch-over trajectories demonstrate that the proposed autopilot performs as intended under aerodynamic uncertainties, as shown in Figure 10c.

V. CONCLUSIONS

This paper proposes a new autopilot structure for agile missiles equipped with jet vanes. The primary objective of this method is to reduce the time response of the attitude controller by utilizing the maximum attitude rate with a Schmitt trigger, particularly during the initial phase immediately after launch, even in low dynamic pressure regions. The controllers for the pitch/yaw and roll channels are designed separately within a skid-to-turn scheme, enabling fast command response. The pitch-over maneuver is managed by autopilots based on a PI attitude controller with a Schmitt trigger, which determines the command direction and uses a pre-calculated maximum angular rate for the command magnitude. Numerical results from a 6-DOF simulation environment demonstrate that the proposed scheme effectively meets mission requirements. Finally, a Monte Carlo simulation is conducted to assess the sensitivity to aerodynamic uncertainties.

REFERENCES

[1] Wise, K. A., and roy, D. J. B., "Agile Missile Dynamics and Control," Journal of Guidance, Control, and Dynamics, Vol. 21, No. 3, 1998, pp.441–449.

[2] Facciano, A. B., Seybold, K. G., Westberry-Kutz, T. L., and Widmer, D. O., "Evolved SeaSparrow Missile Jet Vane Control System Prototype Hardware Development," Journal of Spacecraft and Rockets, Vol. 39, No. 4, 2002, pp. 522–531.

[3] Biberstein, J. X., Tal, E., and Karaman, S., Thrust Vectoring of Small-scale Solid Rocket Motors Using Additively Manufactured Jet Vanes, Proceedings in AIAA Propulsion and Energy 2021 Forum, 2021, p. 3228.

[4] Lee, C.-H., Tahk, M.-J., and Jun, B.-E., "Autopilot design for an agile missile using L1 adaptive backstepping control," Proceedings in 28th Congress of the International Council of the Aeronautical Sciences 2012, Vol. 5, 2012, pp. 3533–3538.

[5] Lee, C.-H., Kim, T.-H., and Tahk, M.-J., "Agile Missile Autopilot Design using Nonlinear Backstepping Control with Time-Delay Adaptation," Transactions of the Japan Society for Aeronautical and Space Sciences, Vol. 57, No. 1, 2014, pp. 9–20.

[6] Mahmood, A., Kim, Y., and Park, J. J., "Robust H autopilot design for agile missile with time-varying parameters," IEEE Transactions on Aerospace and Electronic Systems, Vol. 50, 2014, pp. 3082–3089.

[7] Ryu, S.-M., Won, D.-Y., hun Lee, C., and Tahk, M.-J., "Missile Autopilot Design for Agile Turn Control During Boost-Phase," International Journal of Aeronautical and Space Sciences, Vol. 12, 2011, pp. 365–370.

[8] Menon, P., and Ohlmeyer, E., "Integrated design of agile missile guidance and autopilot systems," Control Engineering Practice, Vol. 9, No. 10, 2001, pp. 1095–1106.

[9] Defu, L., Junfang, F., Zaikang, Q., and Yu, M., "Analysis and improvement of missile three-loop autopilots," Journal of Systems Engineering and Electronics, Vol. 20, No. 4, 2009, pp. 844–851.

[10] Friedland, B., and Williams, D., "Design of autopilots for bank-to-turn missiles," Proceedings in ICCON IEEE International Conference on Control and Applications, 1989, pp. 479–482.

[11] Luo, D., and Chen, B. M., "The autopilot design of bank-to-turn missile using mixed sensitivity H optimization," Proceedings in 2013 IEEE International Conference on Cyber Technology in Automation, Control and Intelligent Systems, 2013, pp. 241–246.

[12] Guo, Z., Zhou, J., and Guo, J., "Robust autopilot design for bank-to-turn missiles using adaptive dual-layer sliding mode control," Optik, Vol. 131, 2017, pp. 383–398.

[13] Nesline, F. W., and Nesline, M. L., "How Autopilot Requirements Constrain the Aerodynamic Design of Homing Missiles," Proceedings in 1984 American Control Conference, 1984, pp. 716–730.